

# The co-localization of HBx and COXIII upregulates COX-2 promoting HepG2 cell growth

BI-YUN ZHENG<sup>1</sup>, XUE-FEN FANG<sup>3</sup>, LAI-YU ZOU<sup>2</sup>, YUE-HONG HUANG<sup>3</sup>, ZHI-XIN CHEN<sup>3</sup>,  
DAN LI<sup>3</sup>, LIN-YING ZHOU<sup>4</sup>, HAO CHEN<sup>5</sup> and XIAO-ZHONG WANG<sup>3</sup>

<sup>1</sup>Graduate School, Fujian Medical University; Departments of <sup>2</sup>Infection and <sup>3</sup>Gastroenterology, Union Hospital of Fujian Medical University; <sup>4</sup>Laboratory of Electron Microscopy, Fujian Medical University, Fuzhou, Fujian 350001; <sup>5</sup>Department of Gastroenterology, The Third Affiliated Hospital of Fujian Medical University, Fuzhou, Fujian 350108, P.R. China

Received March 23, 2014; Accepted May 27, 2014

DOI: 10.3892/ijo.2014.2499

**Abstract.** HBx is a multifunctional regulator that interacts with host factors to contribute to the development of hepatocellular carcinoma. In this study, to explore the co-localization of HBx and COXIII in HepG2 cells and to investigate the molecular mechanism of HBx in HepG2 cell growth promotion, we first constructed a HepG2 cell line stably expressing the HBx gene *in vitro* by lentivirus vectors. In addition, we found that HBx co-localized with the inner mitochondrial protein, COXIII, in HepG2 cells by confocal laser scanning microscopy. It led to changes of mitochondrial biogenesis and morphology, including upregulation of COXIII protein expression, increased cytochrome *c* oxidase activity and higher mitochondrial membrane potential. The upregulation of COX-2 caused by HBx through generation of mitochondrial reactive oxygen species promoted cell growth. Thus, we conclude that co-localization of HBx and COXIII leads to upregulation of COX-2 that promotes HepG2 cell growth. Such a mechanism provides deeper insights into the molecular mechanism of HBV-associated hepatocellular carcinoma.

## Introduction

Hepatocellular carcinoma (HCC) is one of the most common malignant diseases worldwide with the majority of cases relating to hepatitis B virus (HBV) infection. Interactions between the HBV-encoded X (HBx) protein and host factors contribute to the development of HBV-associated HCC (1,2).

HBx is a multifunctional regulator that modulates transcription, signal transduction pathways, cell cycle progression, DNA repair, apoptosis, protein degradation pathways and genetic stability through interaction with host factors (3,4). During recent years evidence has accumulated that HBx protein has both anti-apoptotic and pro-apoptotic actions (5,6). The subcellular localization of HBx is primarily in the cytoplasm, with a small fraction in the nucleus. In addition, a fraction of cytosolic HBx localizes with mitochondria in different cell lines, affecting mitochondrial physiology, metabolism and other relevant functions (7,8). Some research groups have proved that HBx is localized to the outer mitochondrial membrane, consistent with the reported interaction of HBx with the voltage-dependent anion channel (VDAC), a channel that spans the outer mitochondrial membrane (9-11). In recent years, our studies have revealed that HBx can also interact with the inner mitochondrial membrane protein COXIII, by yeast two-hybrid system, mating experiment and coimmunoprecipitation (12,13).

Cytochrome *c* oxidase (COX or complex IV) is the terminal enzyme of the respiratory chain that catalyzes the reduction of molecular oxygen and plays a pivotal role in the generation of ATP and maintenance of mitochondrial membrane potential ( $\Delta\Psi_m$ ) (14,15). COXIII is one of the 3 mtDNA encoded subunits of COX that functions in the process of growth, differentiation, transcription and signal transduction by supporting higher energy requirements for cells (16-18). The effect of cytochrome oxidase decreases when the level of COXIII is reduced (19). COX encoded gene mutations or expression changes may make the cell abnormal that is associated with the development of tumors mainly through an increase in reactive oxygen species in mitochondria oxidative phosphorylation (20-22).

Increasing evidence suggests that inflammation contributes to HCC development due to the adverse effects of inflammatory mediators such as proinflammatory cytokine and reactive oxygen species (ROS). They play a key role on DNA repair, DNA methylation, DNA oxidation and lipid peroxidation (23-25). The main production site of ROS is identified to be mitochondria (26-28). Cyclooxygenase-2 (COX-2) is a key

---

*Correspondence to:* Professor Xiao-Zhong Wang, Department of Gastroenterology, Union Hospital of Fujian Medical University, 29 Xinquan Road, Gulou District, Fuzhou, Fujian 350001, P.R. China  
E-mail: drwangxz@163.com

**Key words:** hepatitis B virus X protein, cytochrome *c* oxidase subunit III, reactive oxygen species, cyclooxygenase-2

mediator of inflammatory responses that promotes the growth of HCC cells by stimulating proliferation, angiogenesis, invasiveness and inhibits apoptosis and immune response (29,30). Notably, there is experimental evidence showing a relationship between ROS and cyclooxygenase-derived products. Thus ROS can promote cyclooxygenase expression and the COX/PG (cyclooxygenase/prostaglandin) synthase pathways can induce the generation of ROS (31). Additionally, ROS from mitochondria plays a key role in COX-2 induction (28,32). However, it remains unknown how the two inflammatory mediators ROS and COX-2 converge during inflammation leading to HCC development.

In this study, we constructed a HepG2 cell line stably expressing the HBx gene by lentivirus vectors to explore the effect of HBx on the development of HBV associated HCC. We found that HBx co-localized with the inner mitochondrial membrane protein, COXIII, leading to changes of mitochondrial biogenesis and morphology. The upregulation of COX-2 caused by HBx through generation of mitochondria ROS promoted cell growth.

## Materials and methods

**Cells cultures.** Human embryonic kidney 293T cell line was provided by ATCC (UK). The human hepatoma cell line HepG2 cell was purchased from Shanghai Cell Bank (Shanghai, China). Cells were cultured in Dulbecco's modified Eagle's medium containing 10% fetal bovine serum and 1% penicillin-streptomycin solution at 37°C in a 5% CO<sub>2</sub> incubator.

**Antibodies and reagents.** Anti-DYKDDDDK-Tag (anti-flag) antibody was purchased from Abmart (Shanghai, China). Anti-COX-2 antibody was purchased from Abcam (Co., USA). Anti-cytochrome *c* oxidase subunit III (anti-COXIII) (N-20) antibody was purchased from Santa Cruz Biotechnology (Santa Cruz, CA). Anti- $\beta$ -actin antibodies were purchased from ZSGB-BIO (Beijing, China). CFTM488-conjugated donkey anti-mouse IgG (H+L), CFTM350-conjugated donkey anti-goat IgG (H+L), N-acetylcysteine (NAC) and puromycin were obtained from Sigma (St. Louis, MO). Mito Tracker Red was obtained from Molecular Probes (Eugene, OR). NS-398 was purchased from Beyotime (Shanghai, China). Cell counting kit-8 was from Dojindo Laboratories (Kumamoto, Japan). Primers were synthesized by Biosune (Shanghai, China).

**Generation of the recombinant lentivirus and establishment of the stably transfected HepG2 cell line.** The HBx expression plasmid PcDNA3.1-x (HBV subtype ayw) was a gift from Professor Michael J. Bouchard (Drexel University College of Medicine, Philadelphia, PA). The lentivirus packaging system: pLOV.CMV.eGFP.2A.EF1a.PuroR (pLOV), psPAX2 and pMD2.G were provided by Neuron Biotech Co., Ltd. (Shanghai, China). The lentivirus vector pLOV contains the gene coding for green fluorescent protein (GFP), puromycin and the peptide DYKDDDDK (flag). Full-length HBx (465 bp) was amplified from PcDNA3.1-x by polymerase chain reaction (PCR) and then infused with flag epitope at the N-terminus and next cloned into pLOV. The recombinant lentiviral particles were generated by transient co-transfection with 293T cells by the three-plasmid expression system, and harvested by filtration

through a 0.45- $\mu$ m filter and ultracentrifugation at 100,000 g for 2 h at 4°C. HepG2 cells at 60% confluency were transfected with the recombinant lentivirus. Then the cell clones were treated with 0.2  $\mu$ g/ml puromycin for 10 days. Positive clones expressing GFP and resistant to puromycin were screened and named HepG2-HBx and HepG2-mock, respectively.

**Indirect immunofluorescence assay.** To eliminate the impact of green fluorescence caused by GFP in HepG2-HBx cells, we used 100% methanol as a fixative. As a result, green fluorescence disappeared (data not shown), consistent with previous research (33). Cells were stained for 30 min with 150 nM Mito Tracker Red and fixed with a 100% ice methanol solution and pre-incubated in blocking solution (5% donkey serum albumin in PBS) and next incubated with primary antibodies (anti-flag, anti-COXIII) at 4°C overnight. Then, the fluorescence-labeled second antibodies (CFTM488-conjugated donkey anti-mouse, CFTM350-conjugated donkey anti-goat) were added and incubated for 60 min at 37°C in the dark, and the sections were mounted using glycerol. Fluorescence images were obtained by confocal laser scanning microscopy (Leica SP5, Solms, Germany).

**Isolation of mitochondria and measurement of COX activity.** Mitochondria were isolated using the mitochondrial isolation kit for mammalian cells (Thermo Scientific, MA, USA) according to the manufacturer's instructions. Briefly, following lysis of approximately  $2 \times 10^7$  cells, cell debris and nuclei were pelleted at 700 x g for 10 min at 4°C, followed by centrifugation at 3,000 x g for 15 min at 4°C to pellet a mitochondria-enriched fraction, and then 12,000 x g for 5 min at 4°C to pellet the isolated mitochondria. Protein concentrations were measured using the bicinchoninic acid (BCA) assay and then adjusted to 1  $\mu$ g/ $\mu$ l. COX activity was determined using the Cytochrome *c* Oxidase Assay kit (GenMed, Shanghai, China) according to the manufacturer's instructions by an enzyme mark instrument (Bio-Tek ELX-800, USA). Isolated mitochondria (10  $\mu$ l) were combined with 10  $\mu$ l of lysis buffer, then mixed with 205  $\mu$ l of buffer solution in 96-well plates. The reaction was initiated by the addition of 25  $\mu$ l of reaction liquid, and the decrease in absorbance at 550 nm was measured for 1 min. Activity was calculated based on the following equation: Units/ml =  $[(\Delta\text{Abs}_{550}/\text{min for the sample} - \Delta\text{Abs}_{550}/\text{min for the blank}) \times \text{dilution factor} \times \text{total reaction volume}] / [\text{mitochondria isolate volume} \times \text{the difference in extinction coefficients between ferro- and ferri-cytochrome } c \text{ at } 550 \text{ nm } (21.84)]$ . One unit is the amount that oxidizes 1  $\mu$ mol reduced cytochrome *c*/min at pH 7.0 and 25°C.

**Flow cytometric analysis.** Cells in the three groups were harvested with trypsin, and resuspended in PBS ( $1 \times 10^6$  cells/ml) for analyzing ROS and mitochondrial membrane potential by flow cytometry (Becton-Dickson Co., C6, San Jose, CA). i) The mitochondrial membrane potential was evaluated using the cationic fluorescent dye TMRM (Sigma). Cells incubated in 100 nM TMRM solution, 20 min at 37°C in the dark, then analysed by a flow cytometer. ii) Intracellular ROS levels were detected by staining cells with 50  $\mu$ M Dihydroethidium (DHE) fluorescence probe (Vigorous Biotechnology, Beijing, China) for 30 min in the dark, then analysed by a flow cytometer.

Table I. Primer sequence for the genes used in RT-PCR analyses.

Gene	Primer sequences	
HBV X (HBx)	Sense:	5'-ATG CAA GCT TAT GGC TGC TAG GCT GTA CTG-3'
	Antisense:	5'-TGC GAA TTC TTA GGC AGA GTG AAA AAG TTG-3'
COXIII	Sense:	5'-AGC CCA TGA CCC CTA ACA-3'
	Antisense:	5'-CCT CAT AGT TAG TGG ACT CG-3'
COX-2	Sense:	5'-TCA AGT CCC TGA GCA TCT ACG-3'
	Antisense:	5'-ACA TTC CTA CCA CCA GCA ACC-3'
$\beta$ -actin	Sense:	5'-GGC ATC GTG ATG GAC TCC G-3'
	Antisense:	5'-GCT GGA AGG TGG ACA GCG A-3'

**Transmission electron microscopy (TEM).** The morphological changes of cell and mitochondria were observed by TEM. A total of  $1 \times 10^6$  of cells were collected and subjected to fixation with 3% fresh glutaraldehyde and 1.5% paraformaldehyde solution at 4°C for 1 h, next to post-fixation with 1% osmium tetroxide and 1.5% potassium ferrocyanide solution at 4°C for 1.5 h, then dehydration was carried out with a graded series of ethanol solution, and finally the cells were to embedded in Epon-618. Ultrathin sections were cut to stain with uranyl acetate and lead citrate, and observed under TEM (Phillips EM208, WI, USA).

**Reverse-transcriptase polymerase chain reaction (RT-PCR) and western blotting.** i) RT-PCR: total RNA was extracted using TRIzol reagent. PCR amplification reactions were set up according to the manufacturer's protocol (Thermo Scientific). The primer sequences of each gene and the PCR conditions are listed in Table I. PCR was carried out in a GeneAmp PCR System (PE2400, USA). The results of electrophoresis were scanned by a UVP scanner with Grab-IT software (Gel Doc 100, Bio-Rad, USA) and gray scale of each band was calculated using Image J software. ii) Western blotting: cells were harvested and cell lysate was prepared. Protein concentration was measured using BCA Protein Assay kit (Beyotime). Immunoblotting was performed using specific primary antibodies then incubated with the appropriate horseradish peroxidase-conjugated secondary antibodies and detected using an ECL kit (ZSGB-BIO). Densitometry was performed on the western blot images by using Image-J software and expressed as arbitrary densitometric units normalised to  $\beta$ -actin expression.

**Cell proliferation assay.** Cell proliferation was analyzed by the cell-counting kit-8. Cells ( $3 \times 10^3$ ) were seeded in 96-well plates and each well contained 100  $\mu$ l of complete DMEM medium (6 replica wells for each cell line). After 1, 2 and 3 days of incubation, the media was removed and 100  $\mu$ l of fresh complete DMEM medium containing premixed CCK-8 (110 dilution in complete DMEM medium) was added to each well. The plates were incubated at 37°C with 5% CO<sub>2</sub> for 3 h, followed by shaking thoroughly for 1 min on a shaker. The absorbance at 450 nm was measured using an ELISA reader, each day of the 3-day experiment to calculate the growth curve.

**Colony formation assay.** Cell suspensions were transferred into 6-well plates (500 cells/well), and each group contained 3 wells. After incubation for 14 days, the cells were rinsed in PBS for twice and stained with Crystal Violet Staining Solution. The experiments were performed in triplicate and the number of colonies containing >50 cells were microscopically counted to calculate the colony formation rate as number of colonies/number of cells x 100%.

**Statistical analysis.** Each set of experiments was repeated at least three times with similar results. Results are expressed as means with standard deviations (SD). Statistical evaluation was carried out by one-way analysis of variance (ANOVA). P-values of <0.05 were considered statistically significant.

## Results

**Establishment of a HepG2 cell line stably expressing the HBx gene.** Lentiviral vectors have become one of the most powerful gene transfer vehicles, they provide several advantages that include being able to transduce a wide range of cell types irrespective of their division status, leading to prolonged transgene expression, lack of pre-existing immunity and less genotoxic (34,35). Our study used lentiviral vectors to establish a HepG2 cell line stably expressing HBx gene *in vitro*. The GFP positive cells were 95-98% by fluorescence microscope (Fig. 1A). Stable expression the HBx mRNA and protein was verified by RT-PCR and western blot, respectively (Fig. 1B). A HepG2 cell line stably transduced with a lentivirus expressing the HBx gene was successfully constructed.

**HBx targets to COXIII leading to changes of mitochondrial biogenesis and morphology in HepG2 cells.** We proceeded with fluorescent staining experiments by a combination of anti-flag antibody, anti-COXIII antibody and a mitochondria-specific staining agent, Mito Tracker Red, then observed cells by confocal microscopy. As indicated in Fig. 2, the staining of HBx protein (green color) together with COXIII protein (blue color) in mitochondria (red color) was observed (white) in HepG2-HBx cells, which suggested that HBx protein co-localized with inner mitochondrial membrane protein COXIII in HepG2 cells, further verifying our previous studies (12,13). Moreover, the localization of HBx was both in the

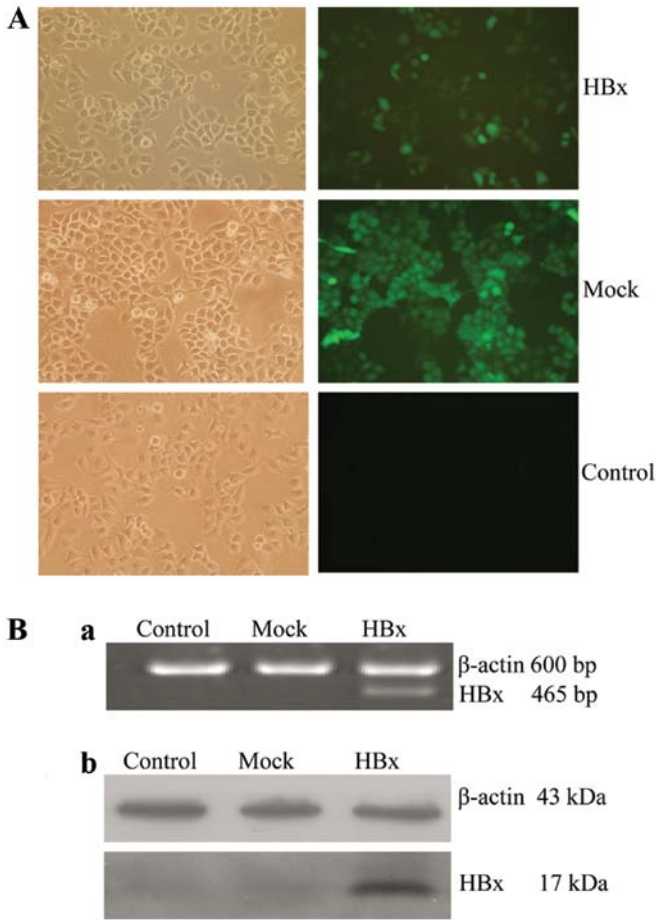


Figure 1. Construction of a HepG2 cell line stably expressing the HBx gene. HBx, Mock and Control represent HepG2-HBx, HepG2-mock and HepG2 cells, respectively. (A) Fluorescence microscope analysis of HepG2 cells transduced with lentiviral vectors expressing green fluorescent protein (GFP). Cells were observed by visible light (left) and fluorescence microscopy (right), respectively (original magnification, x200). (B) Expression of HBx in stably transfected HepG2 cells. (a) RT-PCR detection of HBx mRNA expression. (b) Western blot detection of HBx protein expression by antibody specific against flag protein and  $\beta$ -actin.

nucleus and the cytoplasm, with a fraction of cytosolic HBx in the mitochondria.

Since COXIII is an essential component of the mitochondrial respiratory chain, the co-localization of HBx with COXIII would induce an alteration in the normal mitochondrial function and morphology in HepG2-HBx cells. We found that the protein expression of COXIII was increased in HepG2-HBx cells, while the RNA level did not change as shown in Fig. 3A and B. We then examined the COX activities. Correlating with their upregulated proteins level, they were significantly increased in HepG2-HBx cells compared with HepG2-control and HepG2-mock cells (Fig. 3C). Next, we measured mitochondrial membrane potential ( $\Delta\Psi_m$ ) of cells in the three groups using the fluorochrome TMRM, HepG2-HBx cells displayed the highest  $\Delta\Psi_m$  (Fig. 3D). Increased COXIII protein expression level, upregulation of COX activities as well as the highest  $\Delta\Psi_m$  demonstrated that HBx promoted mitochondrial function in HepG2 cells. To assess the changes of mitochondrial morphology accompanied by the alteration of mitochondrial biogenesis in HepG2-HBx cells, we observed the mitochondria, nuclei and other intracellular membrane structures by TEM. Results showed that only a detectable slight swelling of mitochondria in HepG2-HBx cells was found compared with the other two groups (Fig. 3E). Thus, our studies demonstrated that HBx co-localized with inner mitochondrial protein COXIII in HepG2 cells, leading to the changes of mitochondrial biogenesis and morphology.

*ROS from mitochondria induce the cyclooxygenase-2 gene expression in HepG2-HBx cells.* Mitochondria are major ROS generators, thus changes in mitochondrial function and morphology by HBx would be expected to cause ROS generation in cells (36). We evaluated the ROS level by flow cytometry with the Dihydroethidium (DHE) probe. As shown in Fig. 4A, the ROS generation was the strongest in HepG2-HBx cells compared to the others. Recent studies have shown that ROS from mitochondria is necessary for COX-2

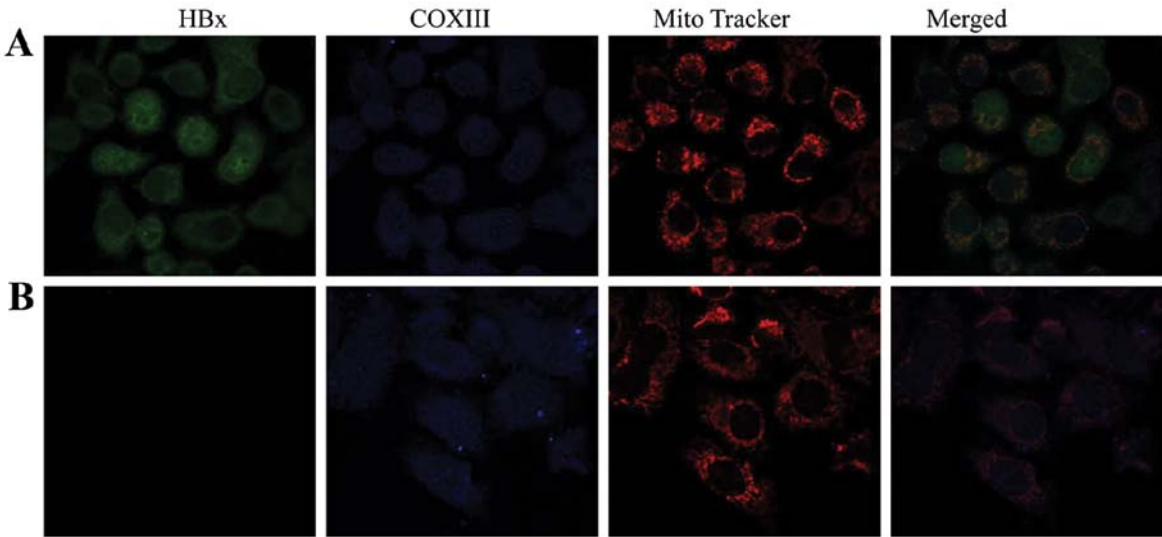


Figure 2. Co-localization of HBx with COXIII in mitochondria by confocal microscopy (original magnification, x800). Subcellular localizations of HBx and COXIII were visualized by immunofluorescence staining with anti-flag antibody (green) and anti-COXIII antibody (blue). Mitochondria were stained with Mito Tracker (red). The merged images are shown in the right panel. (A) HepG2-HBx cells, (B) HepG2 cells.

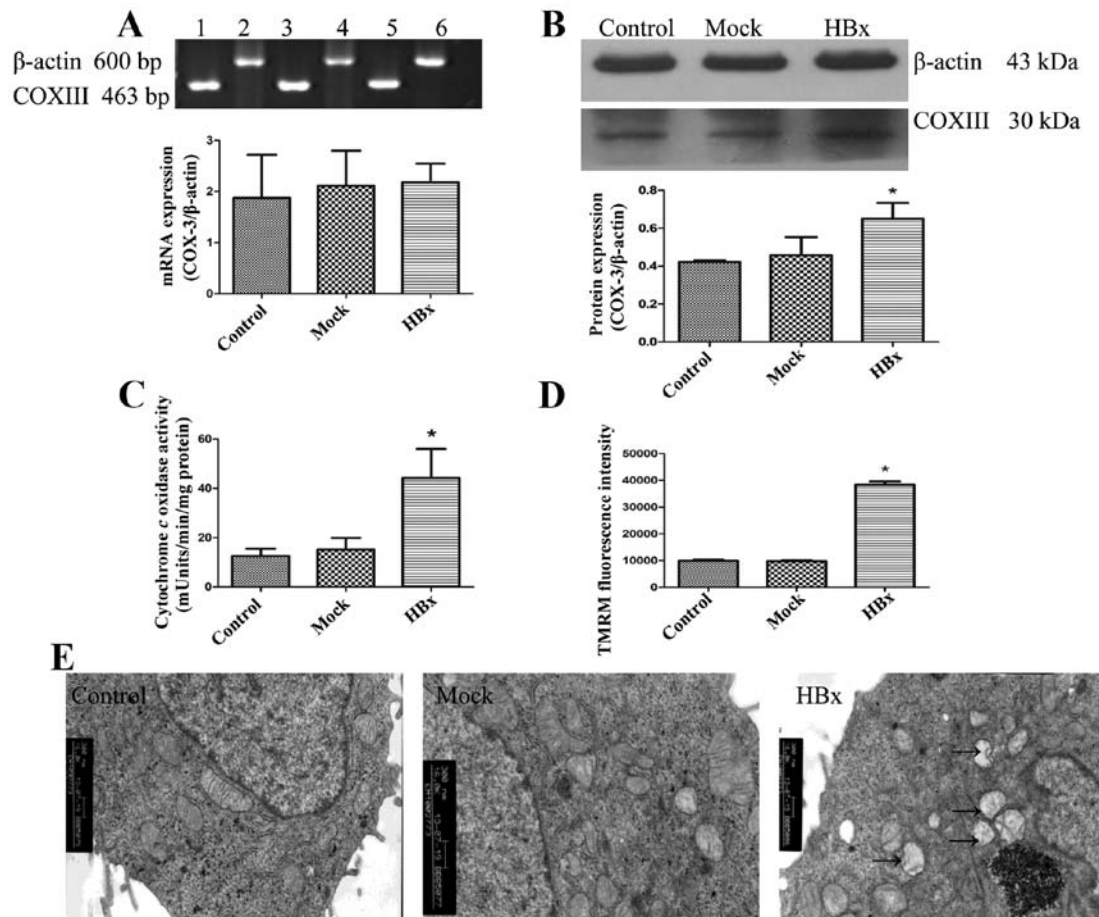


Figure 3. HBx leads to changes of mitochondrial biogenesis and morphology in HepG2 cells. HBx, Mock and Control represent HepG2-HBx, HepG2-mock and HepG2 cells, respectively. (A) Expression of COXIII mRNA was detected using RT-PCR. Lane 1 and 2, 3 and 4-6 represent HepG2, HepG2-mock and HepG2-HBx cells, respectively. (B) Levels of COXIII protein were detected using western blotting by antibody specific against COXIII protein and β-actin. (C) Changes of cytochrome *c* oxidase (COX) activity were determined using the Cytochrome *c* Oxidase Assay kit. (D) Mitochondrial membrane potential was measured by using the fluorescence dye, TMRM, followed by flow cytometry. (E) Morphological changes of mitochondria were examined by electronic microscope (original magnification, x16,000). Arrows show the slight swelling in mitochondria. Values are means ± SD of at least three independent experiments; \*P<0.05.

induction (28,32). We then analyzed whether COX-2 gene expression increased with the ROS generation. Fig. 4B and C show that expression of both COX-2 mRNA and protein was increased in HepG2-HBx cells. To further confirm the notion that ROS from mitochondria induced cyclooxygenase-2 gene expression in HepG2-HBx cells, we treated cells with the antioxidant, N-acetyl cysteine (NAC) (10 mM) for 12 h. As can be seen from Fig. 4D, the induction of COX-2 protein expression by HBx was decreased in HepG2-HBx cells with NAC, but still higher than the other two groups. Therefore, it was clear that ROS from mitochondria induce COX-2 gene expression in HepG2-HBx cells, resulting in inflammatory injury.

**COX-2 promotes the proliferation ability of HepG2 cells.** Substantial research in recent years has demonstrated that HBx promoted cell proliferation associating with HCC in different models and conditions (37,38). To observe the effects of HBx on cell proliferation, we performed the cell viability assay and plate colony formation assay. As shown in Fig. 5A and B, HepG2-HBx cells increased the proliferation rate and formed more colonies, indicating that HBx promoted the proliferation of HepG2 cells. Previous studies have pointed out that COX-2

stimulates proliferation, angiogenesis, invasiveness and inhibits apoptosis to promote the growth of HCC cells (39). We considered that the upregulation of COX-2 contributed to the proliferation mediated by HBx. Further studies were carried out by treating cells with the selective COX-2 inhibitor NS-398 (50 μmol/l) for 72 h. The proliferation of HepG2-HBx cells were significantly suppressed following the inhibition of COX-2 protein expression (Fig. 5C and D). Of note, our data strongly suggest that HBx induced cell proliferation through inflammation.

## Discussion

Hepatocellular carcinoma (HCC) is one of the most common malignant diseases and has the fourth highest cancer mortality rate worldwide. During recent years evidence has accumulated that HBx contributes to the development of HBV-associated HCC (3). The subcellular localization of HBx is primarily cytoplasmic, with a small fraction in the nucleus. In addition, a fraction of cytosolic HBx localizes to the outer mitochondrial membrane in different cell lines, affecting mitochondrial physiology, metabolism and other relevant functions (7-11,40).

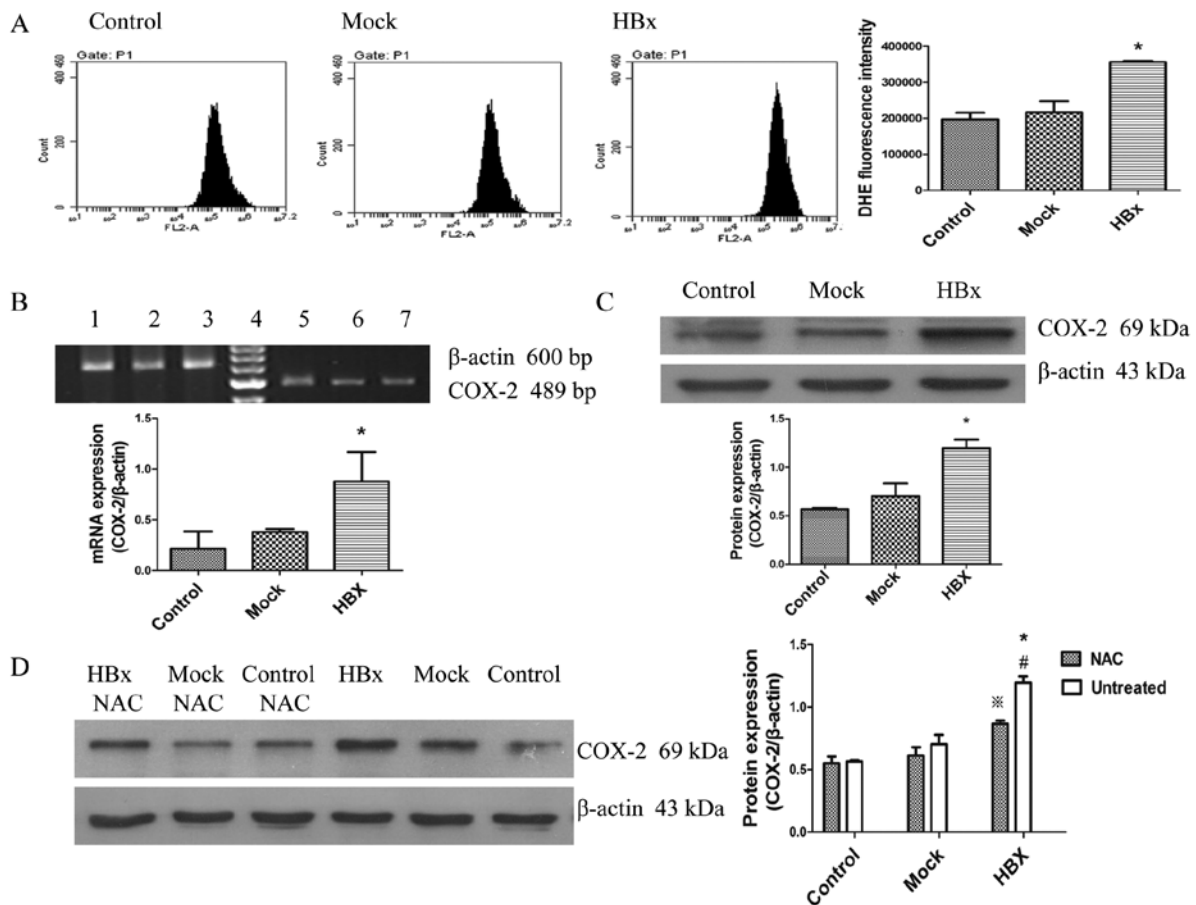


Figure 4. HBx induces ROS generation in HepG2 cells and ROS plays a key role in HBx-induced COX-2 expression. HBx, Mock and Control represent HepG2-HBx, HepG2-mock and HepG2 cells, respectively. (A) HBx increased ROS production in HepG2-HBx cells. Intracellular ROS levels were determined by using the fluorescence dye DHE, followed by flow cytometry. (B) Levels of COX-2 mRNA in cells were detected using RT-PCR. Lane 1 and 5, 2 and 3, 6 and 7 represent HepG2-HBx, HepG2-mock and HepG2 cells, respectively while D is a marker. (C) Levels of COX-2 protein were detected using western blotting by antibody specific against COX-2 protein and  $\beta$ -actin. (D) Western blot analysis for COX-2 protein levels in HepG2-HBx, HepG2-mock and HepG2 cells. Cells in the left three groups were treated with NAC (10 mM) for 12 h. Cells in the right three groups were treated at the same conditions without NAC. Values are means  $\pm$  SD for at least three independent experiments. \* $P$ <0.05 compared with HepG2 and HepG2-mock cells, \*\* $P$ <0.05 compared with HepG2-HBx cells with NAC. # $P$ <0.05 compared with HepG2 and HepG2-mock cells with NAC.

In this study, we successfully constructed a HepG2 cell line stably expressing the HBx gene by lentivirus vectors which can better simulate the progress of chronic hepatitis B virus infection. Then we confirmed the co-localization of HBx with the inner mitochondrial membrane protein COXIII by confocal microscopy in HepG2 cells (Fig. 2), further verifying our previous findings that HBx can also localize to the inner mitochondrial membrane (12,13). The new localization of HBx will give new insight into the role of HBx associated with HCC.

COX plays a pivotal role in the generation and maintenance of mitochondrial membrane potential ( $\Delta\Psi$ m) and ATP (14,15). In this study, to clarify the impact of the co-localization of HBx with COXIII on mitochondrial relevant functions and morphology, we first demonstrated that HBx regulated COXIII gene function at the post-transcription level as the protein expression was increased in HepG2-HBx cells, while the RNA level did not change as shown in Fig. 3A and B. The effect of cytochrome oxidase changed with the alteration of subunit III (19,41). We then found COX activities were significantly increased in HepG2-HBx cells, indicating that

COXIII functions in the process of growth and differentiation, transcription, signal transduction by supporting more energy available for cells (16-18). Next, a higher  $\Delta\Psi$ m was detected in HepG2-HBx cells. TEM results showed a detectable slight swelling in mitochondria of HepG2-HBx cells. Together with the previous findings, we demonstrated that HBx promotes mitochondrial biogenesis in HepG2 cells. Since mitochondria are the key organelles which regulate apoptosis, cellular energetics and signal transduction pathways (42), the alteration of mitochondrial function and morphology may destroy cellular homeostasis.

Several investigators have demonstrated that COX encoded gene expression changes are associated with the development of tumors mainly through increased mitochondrial ROS (20-22,43). A similar increasing trend was observed in our results of mitochondrial ROS as shown in Fig. 4A. HBx increases the level of mitochondrial ROS which is related to hepatocellular carcinogenesis (44,45), but the mechanism remains unclear. Increasing evidence has exposed the relationship between the two main inflammatory mediators, ROS and COX-2 (31). We found that COX-2 gene expression increased

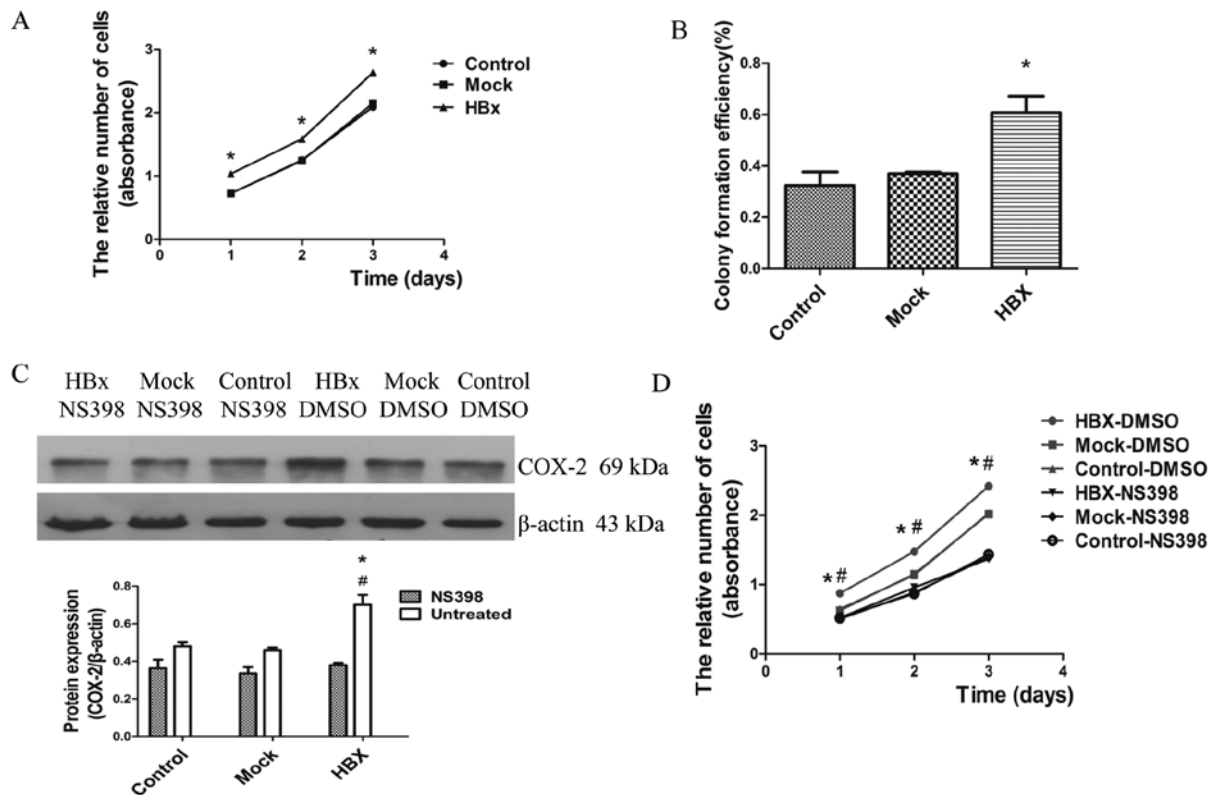


Figure 5. HBx promotes the proliferation ability of HepG2 cells through upregulation of COX-2. HBx, Mock and Control represent HepG2-HBx, HepG2-mock and HepG2 cells, respectively. (A) After incubation for 1, 2 and 3 days, cell proliferation was examined by cell viability assay with cell-counting kit-8 (CCK-8). (B) Colony formation efficiency was detected by plate clone formation assay. After incubation for 2 weeks, the cells were stained with Crystal Violet staining solution and microscopically counted. (C) Western blot analysis for COX-2 protein levels in HepG2-HBx, HepG2-mock and HepG2 cells. Cells in the left three groups were treated with COX-2 inhibitor NS-398 (50  $\mu$ mol/l) for 72 h. Cells in the right three groups were treated with DMSO. (D) Cells were treated with NS-398 (50  $\mu$ mol/l) and DMSO as controls for 72 h, respectively. Following incubation for 1, 2 and 3 days, cell proliferation was examined by Cell viability assay with cell-counting kit-8 (CCK-8). \* $P$ <0.05 compared with HepG2 and HepG2-mock cells, # $P$ <0.05 compared with HepG2-HBx cells with NS398.

with the ROS generation (Fig. 4D). When cells were treated with the antioxidant NAC (10 mM) for 12 h, the induction of COX-2 protein expression by HBx was decreased in HepG2-HBx cells, consistent with previous studies that ROS from mitochondria is necessary for COX-2 induction (28,32). Thus, our work proved that HBx promoted the inflammation in HepG2 cells by generation of mitochondria ROS and led to induction of COX-2, that may contribute to HCC development (23-25).

Research in recent years has demonstrated that inflammation caused by COX-2 stimulates proliferation and inhibits apoptosis to promote the growth of HBx transfected HCC cells (29,39,46). We found HBx promoted cell proliferation by cell viability and plate colony formation assays (Fig. 5A and B). The addition of the selective COX-2 inhibitor NS-398 (50  $\mu$ mol/l) to cells for 72 h significantly suppressed the proliferation of HepG2-HBx cells followed by the inhibition of COX-2 protein expression (Fig. 5C and D). These results strongly indicated that COX-2 mediated HBx promotion of HepG2 cell growth.

All the data above are consistent with the finding that HBx induced cell proliferation through HBx/COXIII/COX-2 pathway. First, we successfully constructed a HepG2 cell line stably expressing the HBx gene by lentivirus vectors. Then we confirmed the co-localization of HBx with the inner mitochondrial membrane protein COXIII leading to the alteration of mitochondrial function and morphology. The upregulation of

COX-2 caused by HBx in HepG2 cells through generation of mitochondria ROS contributed to cell growth. Such a mechanism provides deeper insights into the molecular mechanism of HBV-associated HCC.

## Acknowledgements

This study was supported by the National Natural Science grant 81300321 from the Foundation of China and the Key Clinical Specialty Discipline Construction Program of Fujian, P.R. China (Min Wei Ke Jiao 2012 No. 49). We thank Professor M.J. Bouchard for the pCDNA3.1-X plasmid.

## References

1. Tian Y, Yang W, Song J, Wu Y and Ni B: Hepatitis B virus X protein-induced aberrant epigenetic modifications contributing to human hepatocellular carcinoma pathogenesis. *Mol Cell Biol* 33: 2810-2816, 2013.
2. Xu C, Zhou W, Wang Y and Qiao L: Hepatitis B virus-induced hepatocellular carcinoma. *Cancer Lett* 345: 216-222, 2013.
3. Motavaf M, Safari S, Saffari JM and Alavian SM: Hepatitis B virus-induced hepatocellular carcinoma: the role of the virus x protein. *Acta Virol* 57: 389-396, 2013.
4. Ng SA and Lee C: Hepatitis B virus X gene and hepatocarcinogenesis. *J Gastroenterol* 46: 974-990, 2011.
5. Assrir N, Soussan P, Kremsdorf D and Rossignol JM: Role of the hepatitis B virus proteins in pro- and anti-apoptotic processes. *Front Biosci (Landmark Ed)* 15: 12-24, 2010.



6. Kew MC: Hepatitis B virus x protein in the pathogenesis of hepatitis B virus-induced hepatocellular carcinoma. *J Gastroenterol Hepatol* 26: 144-152, 2011.
7. Rawat S, Clippinger AJ and Bouchard MJ: Modulation of apoptotic signaling by the hepatitis B virus X protein. *Viruses* 4: 2945-2972, 2012.
8. Ma J, Sun T, Park S, Shen G and Liu J: The role of hepatitis B virus X protein is related to its differential intracellular localization. *Acta Biochim Biophys Sin (Shanghai)* 43: 583-588, 2011.
9. Shoshan-Barmatz V, Israelson A, Brdiczka D and Sheu SS: The voltage-dependent anion channel (VDAC): function in intracellular signalling, cell life and cell death. *Curr Pharm Des* 12: 2249-2270, 2006.
10. Rahmani Z, Huh KW, Lasher R and Siddiqui A: Hepatitis B virus X protein colocalizes to mitochondria with a human voltage-dependent anion channel, HVDAC3, and alters its transmembrane potential. *J Virol* 74: 2840-2846, 2000.
11. Clippinger AJ and Bouchard MJ: Hepatitis B virus HBx protein localizes to mitochondria in primary rat hepatocytes and modulates mitochondrial membrane potential. *J Virol* 82: 6798-6811, 2008.
12. Wang XZ, Li D, Tao QM, Lin N and Chen ZX: A novel hepatitis B virus X-interactive protein: cytochrome C oxidase III. *J Gastroenterol Hepatol* 21: 711-715, 2006.
13. Li D, Wang XZ, Yu JP, Chen ZX, Huang YH and Tao QM: Cytochrome C oxidase III interacts with hepatitis B virus X protein in vivo by yeast two-hybrid system. *World J Gastroenterol* 10: 2805-2808, 2004.
14. Mkaouer-Rebai E, Ellouze E, Chamkha I, Kammoun F, Triki C and Fakhfakh F: Molecular-clinical correlation in a family with a novel heteroplasmic Leigh syndrome missense mutation in the mitochondrial cytochrome c oxidase III gene. *J Child Neurol* 26: 12-20, 2011.
15. Bauerfeld CP, Rastogi R, Pirockinaite G, *et al*: TLR4-mediated AKT activation is MyD88/TRIF dependent and critical for induction of oxidative phosphorylation and mitochondrial transcription factor A in murine macrophages. *J Immunol* 188: 2847-2857, 2012.
16. Liang L, Qu L and Ding Y: Protein and mRNA characterization in human colorectal carcinoma cell lines with different metastatic potentials. *Cancer Invest* 25: 427-434, 2007.
17. Bafna S, Singh AP, Moniaux N, Eudy JD, Meza JL and Batra SK: MUC4, a multifunctional transmembrane glycoprotein, induces oncogenic transformation of NIH3T3 mouse fibroblast cells. *Cancer Res* 68: 9231-9238, 2008.
18. Wu H, Rao GN, Dai B and Singh P: Autocrine gastrins in colon cancer cells up-regulate cytochrome c oxidase Vb and down-regulate efflux of cytochrome c and activation of caspase-3. *J Biol Chem* 275: 32491-32498, 2000.
19. Soto IC, Fontanesi F, Valledor M, Horn D, Singh R and Barrientos A: Synthesis of cytochrome c oxidase subunit I is translationally downregulated in the absence of functional F1F0-ATP synthase. *Biochim Biophys Acta* 1793: 1776-1786, 2009.
20. Athar M, Chaudhury NK, Hussain ME and Varshney R: Hoechst 33342 induced reactive oxygen species and impaired expression of cytochrome c oxidase subunit I leading to cell death in irradiated human cancer cells. *Mol Cell Biochem* 352: 281-292, 2011.
21. Bernstein C, Facista A, Nguyen H, *et al*: Cancer and age related colonic crypt deficiencies in cytochrome c oxidase I. *World J Gastrointest Oncol* 2: 429-442, 2010.
22. Gutierrez-Gonzalez L, Graham TA, Rodriguez-Justo M, *et al*: The clonal origins of dysplasia from intestinal metaplasia in the human stomach. *Gastroenterology* 140: 1251-1260, 2011.
23. Szabo G and Lippai D: Molecular hepatic carcinogenesis: impact of inflammation. *Dig Dis* 30: 243-248, 2012.
24. Nishida N, Arizumi T, Takita M, *et al*: Reactive oxygen species induce epigenetic instability through the formation of 8-hydroxydeoxyguanosine in human hepatocarcinogenesis. *Dig Dis* 31: 459-466, 2013.
25. Castello G, Costantini S and Scala S: Targeting the inflammation in HCV-associated hepatocellular carcinoma: a role in the prevention and treatment. *J Transl Med* 8: 109, 2010.
26. Hino K, Hara Y and Nishina S: Mitochondrial reactive oxygen species as a mystery voice in hepatitis C. *Hepatol Res* 44: 123-132, 2014.
27. Indo HP, Inanami O and Koumura T, *et al*: Roles of mitochondria-generated reactive oxygen species on X-ray-induced apoptosis in a human hepatocellular carcinoma cell line, HLE. *Free Radic Res* 46: 1029-1043, 2012.
28. Lim W, Kwon SH, Cho H, *et al*: HBx targeting to mitochondria and ROS generation are necessary but insufficient for HBV-induced cyclooxygenase-2 expression. *J Mol Med (Berl)* 88: 359-369, 2010.
29. Cheng AS, Chan HL, Leung WK, *et al*: Expression of HBx and COX-2 in chronic hepatitis B, cirrhosis and hepatocellular carcinoma: implication of HBx in upregulation of COX-2. *Mod Pathol* 17: 1169-1179, 2004.
30. Bu X and Zhao C: The association between cyclooxygenase-2 1195 G/A polymorphism and hepatocellular carcinoma: evidence from a meta-analysis. *Tumour Biol* 34: 1479-1484, 2013.
31. Hernanz R, Briones AM, Salaices M and Alonso MJ: New roles for old pathways? A circuitous relationship between reactive oxygen species and cyclo-oxygenase in hypertension. *Clin Sci (Lond)* 126: 111-121, 2014.
32. Kiritoshi S, Nishikawa T, Sonoda K, *et al*: Reactive oxygen species from mitochondria induce cyclooxygenase-2 gene expression in human mesangial cells: potential role in diabetic nephropathy. *Diabetes* 52: 2570-2577, 2003.
33. Nybo K: GFP imaging in fixed cells. *Biotechniques* 52: 359-360, 2012.
34. Hu B, Tai A and Wang P: Immunization delivered by lentiviral vectors for cancer and infectious diseases. *Immunol Rev* 239: 45-61, 2011.
35. Liechtenstein T, Perez-Janices N and Escors D: Lentiviral vectors for cancer immunotherapy and clinical applications. *Cancers (Basel)* 5: 815-837, 2013.
36. Lee YI, Hwang JM, Im JH, *et al*: Human hepatitis B virus-X protein alters mitochondrial function and physiology in human liver cells. *J Biol Chem* 279: 15460-15471, 2004.
37. Tang R, Kong F, Hu L, *et al*: Role of hepatitis B virus X protein in regulating LIM and SH3 protein 1 (LASP-1) expression to mediate proliferation and migration of hepatoma cells. *Virol J* 9: 163, 2012.
38. Khattar E, Mukherji A and Kumar V: Akt augments the oncogenic potential of the HBx protein of hepatitis B virus by phosphorylation. *FEBS J* 279: 1220-1230, 2012.
39. Cheng AS, Yu J, Lai PB, Chan HL and Sung JJ: COX-2 mediates hepatitis B virus X protein abrogation of p53-induced apoptosis. *Biochem Biophys Res Commun* 374: 175-180, 2008.
40. Huh KW and Siddiqui A: Characterization of the mitochondrial association of hepatitis B virus X protein, HBx. *Mitochondrion* 1: 349-359, 2002.
41. Hosler JP: The influence of subunit III of cytochrome c oxidase on the D pathway, the proton exit pathway and mechanism-based inactivation in subunit I. *Biochim Biophys Acta* 1655: 332-339, 2004.
42. Salvioi S, Bonafe M, Capri M, Monti D and Franceschi C: Mitochondria, aging and longevity - a new perspective. *FEBS Lett* 492: 9-13, 2001.
43. Ray AM, Zuhlke KA, Levin AM, Douglas JA, Cooney KA and Petros JA: Sequence variation in the mitochondrial gene cytochrome c oxidase subunit I and prostate cancer in African American men. *Prostate* 69: 956-960, 2009.
44. Ha HL and Yu DY: HBx-induced reactive oxygen species activates hepatocellular carcinogenesis via dysregulation of PTEN/Akt pathway. *World J Gastroenterol* 16: 4932-4937, 2010.
45. Lee YI, Hwang JM, Im JH, *et al*: Human hepatitis B virus-X protein alters mitochondrial function and physiology in human liver cells. *J Biol Chem* 279: 15460-15471, 2004.
46. Bae SH, Jung ES, Park YM, *et al*: Expression of cyclooxygenase-2 (COX-2) in hepatocellular carcinoma and growth inhibition of hepatoma cell lines by a COX-2 inhibitor, NS-398. *Clin Cancer Res* 7: 1410-1418, 2001.